influence of the ligand trans to nitrite and that there is a significant cis influence which, for example, causes a regular increase in ^1J(Pt-N) as chloride ligands cis to nitrite are replaced by nitrite. ^1J(Pt-N) for nitrite trans to ammine in our platinum(II) complexes lie in the range 571-613 Hz. From comparison with the results of Kerrison and Sadler[36] and Balch and Wood,[51] the order of trans influence on this coupling constant is $H_2O < Cl^- < Br^- < NH_3 \approx OH^- < NO_2^-$.

It is interesting to note that, for the pair of complexes Pt-$(^{15}NH_3)_3(^{15}NO_2)^+$ and *mer*-Pt$(^{15}NH_3)_3(^{15}NO_2)(OH)_2^+$, the ratio ^1J(Pt(II)-N)/^1J(Pt(IV)-N) is 1.11 for amine trans to nitrite, 1.13 for ammine cis to nitrite, and 1.40 for nitrite. Clearly, all of the variables in eq 1 are not affected to the same extent for the two different types of Pt-N couplings on oxidation by peroxide.

^{15}N-Pt-^{15}N coupling between nonequivalent nitrogen nuclei was observed only between an ammine ^{15}N nucleus and that of a trans nitrite ligand. The coupling constant was larger in platinum(IV) complexes than in their platinum(II) analogues.

(51) Wood, F. E.; Balch, A. L. *Inorg. Chim. Acta* **1983**, *76*, L63.

Acknowledgment. We thank the Australian Research Grants Scheme for financial support. S.F.R. is grateful for receipt of an Australian Commonwealth Postgraduate Scholarship.

Registry No. IV (Z = $^{15}NH_3$), 98857-71-7; IV (Z = H_2O), 98857-72-8; IV (Z = OH^-), 98857-73-9; IV (Z = OSO_3^{2-}), 98857-74-0; IV (Z = Cl^-), 66752-58-7; IV (Z = Br^-), 98857-75-1; IV (Z = I^-), 98857-76-2; IV (Z = $^{15}NO_2^-$), 98857-77-3; IV (Z = Me_2SO-*S*), 66745-15-1; IV (Z = tu), 98857-78-4; IV (Z = SCN^-), 98857-79-5; V (Y = Z = Cl^-), 78017-69-3; V (Y = H_2O, Z = Cl^-), 78039-62-0; V (Y = OH^-, Z = Cl^-), 98874-69-2; V (Y = Z = Br^-), 98857-80-8; V (Y = H_2O, Z = Br^-), 98857-81-9; V (Y = OH^-, Z = Br^-), 98857-82-0; V (Y = Z = I^-), 98857-83-1; V (Y = H_2O, Z = I^-), 98857-84-2; V (Y = Z = $^{15}NO_2$), 98857-85-3; V (Y = H_2O, Z = $^{15}NO_2$), 98857-86-4; V (Y = Z = SCN^-), 98857-87-5; V (Y = H_2O, Z = Me_2SO), 98857-88-6; V (Y = Z = tu), 98857-89-7; VI (Z = $^{15}NH_3$), 98857-90-0; VI (Z = H_2O), 98857-91-1; VI (Z = OH^-), 98839-21-5; VI (Z = Cl^-), 98839-22-6; VI (Z = Br^-), 98839-23-7; VI (Z = I^-), 98839-24-8; VI (Z = $^{15}NO_2^-$), 98839-25-9; VI (Z = SCN^-), 98839-26-0; VI (Z = tu), 98839-27-1; VII (Z = H_2O), 98839-28-2; VII (Z = OH^-), 98839-29-3; VII (Z = Cl^-), 98839-30-6; VII (Z = Br^-), 98839-31-7; VII (Z = I^-), 98839-32-8; VII (Z = $^{15}NO_2^-$), 98839-33-9; VII (Z = SCN^-), 98839-34-0; VII (Z = tu), 98839-35-1; ^{195}Pt, 14191-88-9; ^{15}N, 14390-96-6.

Contribution from the Department of Chemistry, University of Notre Dame, Notre Dame, Indiana 46556

Stereoselectivity in Electron-Transfer Reactions. Determination of the Absolute Configuration of a Nickel Oxime Imine Complex

Daniel P. Martone, Peter Osvath, Charles Eigenbrot, Mauro C. M. Laranjeira,[1a] Robert D. Peacock,[1b] and A. Graham Lappin*

Received August 8, 1985

The crystal structure of the stereospecifically formed complex $[Ni^{II}((S)\text{-}Me_2LH_2)](ClO_4)_2$, where (*S*)-$Me_2LH_2$ is a chiral sexidentate bis(oxime imine) ligand, has been determined. It crystallizes in orthorhombic space group $P2_12_12_1$ (No. 19), with Z = 4, a = 14.817 (2) Å, b = 18.864 (2) Å, c = 9.269 (1) Å, and R = 0.063 for 2502 reflections. The absolute configuration around the metal center in $[Ni^{II}((S)\text{-}Me_2LH_2)]^{2+}$ is ΛΔΛΔΛΔ, abbreviated Λ. In the reduction of [Λ-Ni^{IV}((*S*)-Me_2L)]$^{2+}$ by $[Co(pdta)]^{2-}$ and $[Co(cdta)]^{2-}$, the products show an excess of $[\Delta\text{-}Co(pdta)]^-$ and $[\Delta\text{-}Co(cdta)]^-$, respectively, of approximately 10%. Comparable results have been obtained for [Λ-Ni^{III}((*S*)-Me_2LH)]$^{2+}$ reduction. This chiral induction is explained in terms of stereoselectivity in precursor complex formation supported by ion-exchange studies which reveal that the ion pair [Λ-$Ni^{IV}L^{2+}$,Δ-$Co(edta)^-$] is preferred over [Δ-$Ni^{IV}L^{2+}$, Δ-$Co(edta)^-$], where LH_2 is a nonchiral analogue of (*S*)-Me_2LH_2. These stereochemical studies and kinetic studies have been used to produce a detailed picture of the electron-transfer precursor complex.

Introduction

The study of stereoselectivity in outer-sphere electron-transfer reactions between metal ion complexes in solution has the potential for yielding valuable information about the interactions between the participating species. Well-defined examples of stereoselectivity have been reported by a number of authors;[2-6] however, the data available provide no basis for predicting the extent and course of the stereochemical induction and detailed interpretation has not been possible.

The extent of chiral induction is generally small but may be measured by the detection of optical activity in the products of reaction between an optically active complex and a racemic mixture, provided proper amount is taken of the racemization of the reactants or reaction products by a self-exchange electron-transfer mechanism.[2,3] This latter problem and the fact that kinetic methods for determining stereoselectivity lack the necessary sensitivity continue to confound studies in this area.[7-13]

A useful strategy in preventing racemization by a self-exchange electron-transfer pathway involves the use of chiral ligands which complex with metal ions in a stereospecific fashion. The ligand (5*S*,12*S*)-4,7,10,13-tetraaza-3,5,12,14-tetramethylhexadeca-3,13-diene-2,15-dione dioxime, (*S*)-Me_2LH_2 (**1**), is a chiral analogue of the sexidentate ligand 3,14-dimethyl-4,7,10,13-tetraazahexadeca-3,13-diene-2,15-dione dioxime, LH_2 (**2**), and complexes stereospecifically with nickel(II).[6] This can be oxidized to both nickel(III) and nickel(IV) forms, with retention of configuration.

(1) (a) Permanent address: Department of Chemistry, Universidade Federal de Santa Catarina, Florianopolis, Santa Catarina, 88000, Brasil. (b) Permanent address: Department of Chemistry, University of Glasgow, Glasgow, G12 8QQ Scotland, U.K.
(2) Geselowitz, D. A.; Taube, H. *J. Am. Chem. Soc.* **1980**, *102*, 4525-4526.
(3) Kondo, S.; Sasaki, Y.; Saito, K. *Inorg. Chem.* **1981**, *20*, 429-433.
(4) Porter, G. B.; Sparks, R. H. *J. Chem. Soc., Chem. Commun.* **1979**, 1094-1095.
(5) Kaizu, Y.; Mori, T.; Kobayashi, H. *J. Phys. Chem.* **1985**, *89*, 332-335.
(6) Lappin, A. G.; Laranjeira, M. C. M.; Peacock, R. D. *Inorg. Chem.* **1983**, *22*, 786-791.
(7) Grossman, B.; Wilkins, R. G. *J. Chem. Soc.* **1967**, *89*, 4230-4232.
(8) Sutter, J. H.; Hunt, J. B. *J. Am. Chem. Soc.* **1969**, *91*, 3107-3108.
(9) Kane-Maguire, N. A. P.; Tollison, R. M.; Richardson, D. E. *Inorg. Chem.* **1976**, *15*, 499-500.
(10) Blinn, E. L.; Wilkins, R. G. *Inorg. Chem.* **1976**, *15*, 2952.
(11) Geue, R. J.; McCarthy, M. G.; Sargeson, A. M. *J. Am. Chem. Soc.* **1984**, *106*, 8282-8291.
(12) Armstrong, R. A.; Sykes, A. G. *J. Am. Chem. Soc.* **1978**, *100*, 7710.
(13) Toma, H. E.; Murakami, R. A. *Inorg. Chim. Acta* **1984**, *93*, L33-L36.

0020-1669/85/1324-4693$01.50/0

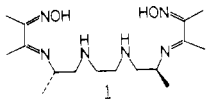

1

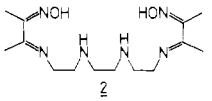

2

Chiral induction of approximately 10% has been observed[6] in the oxidation of $[Co(edta)]^{2-}$ by the nickel(IV) complex $[Ni^{IV}((S)\text{-}Me_2L)]^{2+}$. The complex $[Co(edta)]^{2-}$ is an ideal probe for stereoselectivity studies as the cobalt(III/II) self-exchange rate is low;[14] however, interpretation of stereoselectivity data presents a problem because the complex has low symmetry. In this paper, kinetic and stereoselectivity studies are extended to include the nickel(IV) oxidations of the substituted derivatives $[Co(pdta)]^{2-}$ and $[Co(cdta)]^{2-}$ in an attempt to define the orientation of the reactant complexes during the electron-transfer process. The stereoselectivity of the ion-pairing interaction between the nickel(IV) complexes and $[Co(edta)]^{-}$ has been examined and the absolute configuration of $[Ni^{II}((S)\text{-}Me_2LH_2)]^{2+}$ determined by X-ray crystallography.

Experimental Details

(a) Preparation of Complexes. The complexes $[Ni^{II}LH_2](ClO_4)_2$ and $[Ni^{IV}L](ClO_4)_2$ were prepared as outlined previously.[15,16] Synthesis of the chiral ligand (*S*)-Me_2LH_2 was achieved by the published procedure.[6] Crystals of $[Ni^{II}((S)\text{-}Me_2LH_2)](ClO_4)_2$ suitable for diffraction studies were obtained by the addition of a stoichiometric amount of (*S*)-Me_2LH_2 to a warmed and stirred solution of nickel(II) perchlorate hexahydrate in ethanol, followed by recrystallization from hot water. Solutions of $[Ni^{IV}((S)\text{-}Me_2L)]^{2+}$ were prepared by oxidation of solutions of $[Ni^{II}((S)\text{-}Me_2LH_2)]^{2+}$ by a small excess of $[IrCl_6]^{2-}$, followed by separation with an anion-exchange resin. Solutions of $[Ni^{III}((S)\text{-}Me_2L)]^{+}$ were prepared by mixing of equimolar amounts of $[Ni^{IV}((S)\text{-}Me_2L]^{2+}$ and $[Ni^{II}((S)\text{-}Me_2LH_2)]^{2+}$ and adjusting the solutions to pH ~5.

The complexes (1,2-diaminopropane-*N*,*N*,*N'*,*N'*-tetraacetato)cobaltate(II), $[Co(pdta)]^{2-}$, and (1,2-diaminocyclohexane-*N*,*N*,*N'*,*N'*-tetraacetato)cobaltate(II), $[Co(cdta)]^{2-}$, were prepared by the addition of a 10% excess of the ligands H_4pdta and H_4cdta (Sigma) to a previously standardized solution of cobalt(II) nitrate (BDH, AnalaR, or Baker Analyzed) followed by addition of 2 equiv of base. The sodium salt of $\Delta(+)_{546}$-(1,2-diaminoethane-*N*,*N*,*N'*,*N'*-tetraacetato)cobaltate(III) was prepared as described by Gillard and co-workers.[17]

(b) X-ray Crystallography. A red-brown irregular crystal of $[Ni^{II}((S)\text{-}Me_2LH_2)](ClO_4)_2$ having approximate dimensions of 0.20 × 0.30 × 0.30 mm was mounted in a glass capillary in a random orientation. Preliminary examination and data collection were performed on an Enraf-Nonius CAD4 diffractometer. Axial photographs confirmed the axial lengths and the Laue class. Cell parameters were determined by the least-squares refinement of 25 reflections between 22 and 30° in 2θ (Mo Kα, λ = 0.71073 Å). A summary of the crystal data and intensity collection parameters is presented in Table I.

All calculations were performed with use of SDP-PLUS.[18] A total of 4304 $+h,+k,+l$ reflections were collected, of which 4276 were not systematically absent. The standard deviation on intensities is $\sigma^2(F_o^2) \alpha \sigma_c^2 + (pF_o^2)^2$, where σ_c is from counting statistics and p (=0.04) is introduced to downweight intense reflections. The intensities of three standard reflections remained constant within experimental error throughout data collection. No decay correction was applied.

Lorentz and polarization corrections were applied to the data. The linear absorption coefficient is 10.2 cm^{-1} for Mo Kα radiation. Azimuthal scans of five reflections with 2θ between 4 and 50° revealed transmission factors between 0.95 and 1.00. No absorption correction was made.

Table I. Summary of Crystal Data and Intensity Collection Parameters for $[Ni^{II}((S)\text{-}Me_2LH_2)](ClO_4)_2$

T, K	294
formula	$NiCl_2O_{10}N_6C_{16}H_{32}$
fw	598.08
cryst dimens, mm	0.21 × 0.30 × 0.19
space group	$P2_12_12_1$
a, Å	14.817 (2)
b, Å	18.864 (2)
c, Å	9.269 (1)
V, Å^3	2590.9
Z	4
density (calcd), g/cm^3	1.533
density (obsd), g/cm^3	1.537
radiation	graphite-monochromated Mo Kα (λ = 0.71073 Å)
scan technique	θ–2θ
ω scan range, deg	0.6 + 0.35 tan θ
2θ scan rate, deg/min	2.6–8.0
bkgd	additional 25% on each extreme of scan
2θ limit, deg	4.0–60.4
criterion for observn	$F_o^2 > 3.0\sigma(F_o^2)$
unique observed data	2502
μ(Mo Kα), cm^{-1}	10.2
R_1 ($\sum\|\|F_o\| - \|F_c\|\|/\sum\|F_o\|$)	0.063
R_2 ($\sum w(\|F_o\| - \|F_c\|)^2/\sum wF_o^2$)	0.072
goodness of fit	1.98
data/parameter	8.45

The structure was solved by direct methods, which revealed the nickel and two chlorine atoms. Remaining atoms were located in succeeding difference Fourier syntheses. The absolute configuration around the metal center was assigned from knowledge of the configuration of the ligand. The two perchlorate anions exhibit disorder that was described with use of 2 chlorine and 3 oxygen atoms at unit occupancy and 10 oxygen atoms at half-occupancy. The disorder in perchlorate 1 mostly involves two oxygens, while that in perchlorate 2 involves rotation about the local pseudothreefold axis. All heavy atoms except the perchlorate oxygens were refined with anisotropic thermal parameters. Hydrogen atoms were included in calculated positions for all but those on the oxime oxygen atoms with isotropic thermal parameters of 6.0 Å^2, but no hydrogens were refined in any way.

Scattering factors were taken from Cromer and Waber.[19] Anomalous dispersion effects were included in F_c;[20] the values were those of Cromer.[21] Only the 2502 reflections with $F_o^2 > 3.0\sigma(F_o^2)$ were used in the refinements. The final cycle of refinement included 296 variable parameters and converged with unweighted and weighted agreement; R_1 = 0.063 and R_2 = 0.072. At convergence, the largest shift was 0.20σ. Outside the perchlorate anions, the largest shift was 0.04σ. The standard deviation of an observation of unit weight was 1.98. The highest peak in the final difference Fourier had a height of 0.75 e/Å^3 with an estimated error based on ΔF[22] of 0.10 e/Å^3 and was 0.7 Å from O7′. Of the top 20 difference peaks, 17 were 1 Å, or less from a perchlorate oxygen atom. Refinement of the opposite enantiomer led to R factors of 0.069 and 0.078. The probability that this enantiomer is correct is less than 0.5% by the Hamilton R-factor ratio test. The residuals showed the poorest agreement in the low-angle data, probably due to the moderate adequacy of the perchlorate disorder model.

(c) Chromatographic Experiments. Samples of the racemic nickel(IV) complex $[Ni^{IV}L]^{2+}$ were absorbed as a 2-mm band on a 100 mm × 10 mm (i.d.) column of Dowex 50X2-400 cation-exchange resin. The sample was eluted (5 days) with a solution of $Na^+[\Delta(+)_{546}\text{-}Co(edta)]^-$ (0.10 M) containing sodium perchlorate (0.10 M), recycled with use of a peristaltic pump. After the band had spread to over 20 mm, the column was washed with 10^{-4} M $HClO_4$ and the resin containing the nickel(IV) complex was divided into seven sections, removed sequentially. $[Ni^{IV}L]^{2+}$ was removed for each section of resin with use of 2 M $NaClO_4$ and the circular dichroism spectrum of each sample recorded.

(d) Kinetic Measurements. The kinetics of reduction of $[Ni^{IV}L]^{2+}$ by $[Co(pdta)]^{2-}$ and by $[Co(cdta)]^{2-}$ were investigated under pseudo-first-

(14) Im, Y. A.; Busch, D. H. *J. Am. Chem. Soc.* **1961**, *83*, 3357–3362.
(15) Mohanty, J. G.; Singh, R. P.; Chakravorty, A. *Inorg. Chem.* **1975**, *14*, 2178–2183.
(16) Lappin, A. G.; Laranjeira, M. C. M. *J. Chem. Soc., Dalton Trans.* **1982**, *1861*–1865.
(17) Gillard, R. D.; Mitchell, P. R.; Weick, C. F. *J. Chem. Soc., Dalton Trans.* **1974**, 1635–1636.
(18) Frenz, B. A. In "Computing in Crystallography"; Schenk, H., Olthof-Hazelkamp, R., van Konigsveld, H., Bassi, G. C., Eds.; Delft University Press: Delft, Holland, 1978; pp 64–71.
(19) Cromer, D. T.; Waber, J. T. "International Tables For X-ray Crystallography"; Kynoch Press: Birmingham, England, 1974; Vol. IV, Table 2.2B.
(20) Ibers, J. A.; Hamilton, W. C. *Acta Crystallogr.* **1964**, *17*, 781–782.
(21) Cromer, D. T. "International Tables for X-ray Crystallography"; Kynoch Press: Birmingham, England, 1974; Vol. IV, Table 2.3.1.
(22) Cruikshank, D. W. J. *Acta Crystallogr.* **1949**, *2*, 154–157.

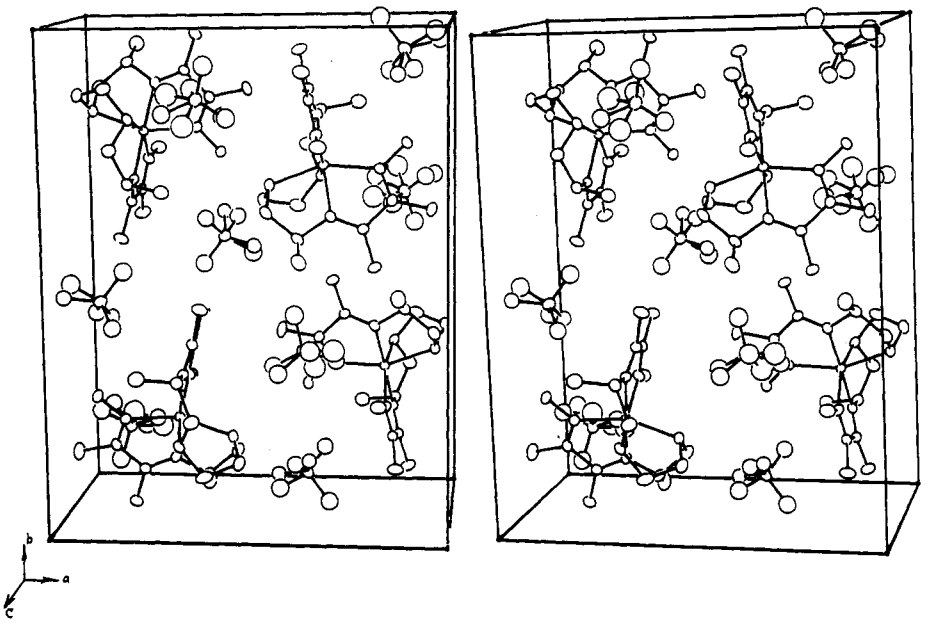

Figure 1. Stereoscopic view of the molecular packing of $[Ni^{II}((S)\text{-}Me_2LH_2)](ClO_4)_2$. Thermal ellipsoids are drawn at the 20% level.

order conditions with an excess of reductant in the presence of 1.5×10^{-2} M buffer at 0.10 M ionic strength ($NaNO_3$). Both reactions are biphasic in nature, similar to the reduction by $[Co(edta)]^{2-}$.[6] The initial phase, nickel(IV) reduction, was monitored at 500 nm under pH conditions where the second phase is very slow and does not interfere. The second phase, nickel(III) reduction, increases in rate with decreasing pH was monitored over the appropriate time scale at 391 nm, an isosbestic point for the initial phase, around pH 4, where disproportionation reactions do not compete.[6]

An Applied Photophysics stopped-flow spectrophotometer thermostated at 25.0 ± 0.1 °C was used. Reactions showed good first-order behavior, and observed rate constants were evaluated by least-squares analysis of appropriate plots with a P.E.T. 2001 microcomputer. Normally, three rate determinations were made for each kinetic experiment.

The pH of solutions was determined immediately after reaction with an E.I.L. 7055 pH meter. Other pH measurements were made with a Beckman Select Ion 2000 meter. A saturated calomel (NaCl) reference electrode was used, and hydrogen ion concentrations were evaluated by using the relationship $-\log [H^+] = pH - 0.02$, correcting for both hydrogen ion activity and the liquid-junction potential.

(e) Stereoselectivity Studies. Stereoselectivities in the reductions of $[Ni^{IV}((S)\text{-}Me_2L)]^{2+}$ and $[Ni^{III}((S)\text{-}Me_2LH)]^{2+}$ by excess $[Co(pdta)]^{2-}$ and $[Co(cdta)]^{2-}$ were determined by measuring the optical activity of the cobalt(III) complexes produced in the reaction. After the reactions had gone to completion, the product solutions were passed through a cation-exchange resin (Amberlite IR-20) in the sodium form to remove optically active nickel(II) species. Identical results were obtained with use of the anion-exchange workup procedures outlined previously.[6]

Stereoselectivity results are quoted as $\Delta\epsilon_{obsd}/\Delta\epsilon_{lit.}$ for the cobalt(III) species.[23] Circular dichroism spectra were measured on an Aviv circular dichroism spectropolarimeter, Model 60DS (Aviv Associates, Lakewood, NJ), calibrated against an aqueous solution of $[\Lambda(+)\text{-}Co(en)_3]Cl_3$ ($\Delta\epsilon_{493} = 1.90\ M^{-1}\ cm^{-1}$).[24]

Visible spectra were run on a Varian D.M.S. 100 spectrophotometer.

Results and Discussion

In an assessment of the implications of stereoselectivity in electron-transfer reactions, a knowledge of the absolute configurations of the species involved is a distinct advantage. Accordingly, the absolute configuration of $[Ni^{II}((S)\text{-}Me_2LH_2)]^{2+}$ has been determined by X-ray crystallography. Since the ligand $(S)\text{-}Me_2LH_2$ complexes with both nickel(II) and nickel(IV) stereospecifically,[6] and since these species are readily and reversibly interconvertible, the absolute configuration of the nickel(II) complex defines the absolute configuration of the nickel(III) and nickel(IV) states also.

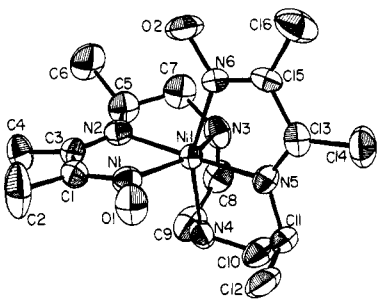

Figure 2. ORTEP diagram of the $[Ni^{II}((S)\text{-}Me_2LH_2)]^{2+}$ ion illustrating the numbering scheme. The thermal ellipsoids are drawn at the 50% level.

(a) Description of the Structure of $[Ni^{II}((S)\text{-}Me_2LH_2)](ClO_4)_2$. The crystal structure consists of discrete molecular ions at general positions in the unit cell (Figure 1). There is one nickel complex cation and two perchlorate anions per asymmetric unit. The closest interion, nonbonded contact is 2.70 Å between O1 and O4, and there are several other hydrogen-bonding interactions between perchlorate oxygen atoms and the metal complex, involving both oxime oxygens and nitrogens N3 and N4. The seven hydrogen-bonding distances less than 3.25 Å are listed in Table II.

The molecular cation consists of a nickel(II) ion in a severely distorted octahedral environment provided by the six nitrogens of the oxime imine ligand (Figure 2). The N–Ni–N angles that are nominally 90° range from 76.1 (2) to 102.3 (2)°, while those nominally 180° range from 155.3 (2) to 177.2 (2)°. Other evidence of constraints placed on the ligand by its coordination to the nickel ion include the interior angles at carbons C1, C3, C13, and C15 which are ≥5° less than 120°. However, in comparison with the closely related complex $[Ni^{II}LH_2](ClO_4)_2$,[25] the principal conclusion is of the preponderant similarity between the two complexes. To aid in this comparison, some pertinent numbers from the earlier work are included in Tables II and III. The Ni–N distances average 2.082 (48) Å in the present study vs. 2.074 (55) Å in the previous work, where the number in parentheses is the variance in the average. Elsewhere in the ligand, bond lengths and angles are very similar, mostly equal within experimental error. Atomic positions and their estimated standard deviations are presented in Table IV.

(b) Absolute Configuration of $[Ni^{II}((S)\text{-}Me_2LH_2)]^{2+}$. The ligand $(S)\text{-}Me_2LH_2$ contains two chiral centers of known, *S*, configu-

(23) Brennan, B. J.; Igi, K.; Douglas, B. E. *J. Coord. Chem.* **1974**, *4*, 19–26.
(24) McCaffery, A. J.; Mason, S. F.; Norman, B. J.; Sargeson, A. M. *J. Chem. Soc. A* **1968**, 1304–1310.
(25) Korvenranta, J.; Saarinen, H.; Näsäkkälä, M. *Inorg. Chem.* **1982**, *21*, 4296–4300.

Table II. Bond Distances (Å) in $[Ni^{II}((S)\text{-}Me_2LH_2)](ClO_4)_2$[a]

atom 1	atom 2	dist this work	dist ref 25	atom 1	atom 2	dist this work	dist ref 25
			Bond Distances				
Ni1	N1	2.105 (5)	2.106 (4)	O1	N1	1.396 (6)	1.384 (4)
Ni1	N2	2.047 (5)	2.008 (3)	O2	N6	1.390 (6)	1.386 (5)
Ni1	N3	2.144 (5)	2.101 (4)	N1	C1	1.280 (7)	1.284 (5)
Ni1	N4	2.106 (5)	2.095 (3)	N2	C3	1.275 (7)	1.272 (6)
Ni1	N5	2.010 (5)	2.001 (3)	N2	C5	1.470 (8)	1.467 (5)
Ni1	N6	2.082 (5)	2.131 (5)	N3	C7	1.488 (9)	1.488 (6)
O7	O8′	1.67 (2)		N3	C8	1.462 (9)	1.484 (6)
C1	C3	1.485 (8)		N4	C9	1.471 (9)	1.485 (6)
C1	C2	1.498 (8)		N4	C10	1.472 (8)	1.481 (5)
C3	C4	1.466 (8)		N5	C11	1.473 (8)	1.464 (6)
C5	C6	1.507 (11)		N5	C13	1.262 (8)	1.273 (3)
C5	C7	1.508 (10)		N6	C15	1.282 (8)	1.279 (5)
C8	C9	1.506 (10)		C10	C11	1.525 (9)	1.524 (6)
C11	C12	1.505 (9)		C13	C14	1.526 (9)	1.487 (7)
C13	C15	1.507 (10)		C15	C16	1.468 (9)	1.492 (6)
Cl1	O3	1.431 (7)		Cl1	O4	1.402 (7)	
Cl1	O5	1.35 (2)		Cl1	O5′	1.515 (15)	
Cl1	O6	1.465 (14)		Cl1	O6′	1.29 (2)	
Cl2	O7	1.39 (2)		Cl2	O7′	1.35 (2)	
Cl2	O8	1.33 (2)		Cl2	O8′	1.44 (2)	
Cl2	O9	1.399 (9)		Cl2	O10	1.42 (2)	
Cl2	O10′	1.395 (15)					
			Hydrogen-Bonding Distances Less Than 3.25 Å				
O1	O4	2.70		O2	O10	3.00	
O2	O10′	2.86		O7′	N3	3.02	
O7	N3	3.09		O8	N3	2.87	
O8′	N4	3.14					

[a] Numbers in parentheses are estimated standard deviations in the least significant digits. Data from ref 25 refer to $[Ni^{II}LH_2]^{2+}$.

Table III. Bond Angles (deg) in $[Ni^{II}((S)\text{-}Me_2LH_2)](ClO_4)_2$[a]

atoms	angle this work	angle ref 25	atoms	angle this work
N1-Ni1-N2	76.1 (2)	76.2	N1-C1-C3	114.1 (5)
N1-Ni1-N3	155.3 (2)	159.1	C2-C1-C3	122.0 (6)
N1-Ni1-N4	98.7 (2)	98.0	N1-C1-C2	123.8 (6)
N1-Ni1-N5	102.3 (2)	104.1	N2-C3-C1	115.0 (5)
N1-Ni1-N6	93.2 (2)	86.1	C1-C3-C4	118.1 (6)
N2-Ni1-N3	79.8 (2)	82.6	N2-C3-C4	126.8 (6)
N2-Ni1-N4	101.0 (2)	98.0	N2-C5-C7	106.6 (5)
N2-Ni1-N5	177.2 (2)	179.0	N2-C5-C6	113.2 (7)
N2-Ni1-N6	101.0 (2)	105.1	C6-C5-C7	110.9 (7)
N3-Ni1-N4	80.5 (2)	84.1	N3-C7-C5	112.0 (6)
N3-Ni1-N5	102.0 (2)	96.9	N3-C8-C9	112.0 (6)
N3-Ni1-N6	96.7 (2)	99.8	N4-C9-C8	110.5 (6)
N4-Ni1-N5	81.5 (2)	82.3	N4-C10-C11	111.1 (6)
N4-Ni1-N6	156.9 (2)	158.2	C10-C11-C12	113.4 (6)
N5-Ni1-N6	76.7 (2)	75.9	N5-C11-C12	109.7 (5)
N5-C11-C10	105.9 (6)		N5-C13-C14	125.9 (7)
C14-C13-C15	119.1 (7)		N5-C13-C15	115.0 (6)
N6-C15-C13	112.8 (6)		N6-C15-C16	125.6 (7)
C13-C15-C16	121.6 (7)		O1-N1-C1	114.0 (5)
C3-N2-C5	125.1 (6)		C7-N3-C8	113.4 (5)
C9-N4-C10	110.6 (6)		C11-N5-C13	125.7 (6)
O2-N6-C15	115.1 (5)		O7-Cl2-O10	108 (1)
O3-Cl1-O4	105.3 (4)		O7′-Cl2-O9	98.1 (8)
O3-Cl1-O5	117.8 (8)		O7′-Cl2-O10′	118.6 (9)
O3-Cl1-O5′	105.7 (6)		O7-Cl2-O9	119.9 (7)
O5′-Cl1-O6′	111 (1)		O8-Cl2-O9	107.0 (9)
O4-Cl1-O5	114.3 (8)		O8′-Cl2-O9	102.9 (8)
O4-Cl1-O6	97.9 (6)		O8′-Cl2-O10′	102.2 (9)
O5-Cl1-O6	105.2 (9)		O9-Cl2-O10	110.0 (9)
O4-Cl1-O5′	101.3 (6)		O8-Cl2-O10	101 (1)
O3-Cl1-O6	114.7 (6)		O7′-Cl2-O8′	121 (1)
O3-Cl1-O6′	97.3 (8)		O7-Cl2-O8	110 (1)
O4-Cl1-O6′	134 (1)		O9-Cl2-O10′	113.4 (8)

[a] Numbers in parentheses are estimated standard deviations in the least significant digits. Data from ref 25 refer to $[Ni^{II}LH_2]^{2+}$.

rations and wraps around the nickel(II) ion to define a further chiral center. The absolute configuraion around the metal can be related to the absolute configuration of the carbon centers on the ligand and is designated[26] ΛΔΛΛΔΛ as shown in Figure 2. It will be abbreviated as Λ. This absolute configuraion is assigned to the corresponding nickel(III) and nickel(IV) complexes, and circular dichroism spectra of $[\Lambda\text{-}Ni^{IV}((S)\text{-}Me_2L)]^{2+}$ and $[\Lambda\text{-}Ni^{III}((S)\text{-}Me_2L)]^{+}$ are shown in Figure 3, while the spectra of $[\Lambda\text{-}Ni^{II}((S)\text{-}Me_2LH_2)]^{2+}$ are presented in Figure 4.

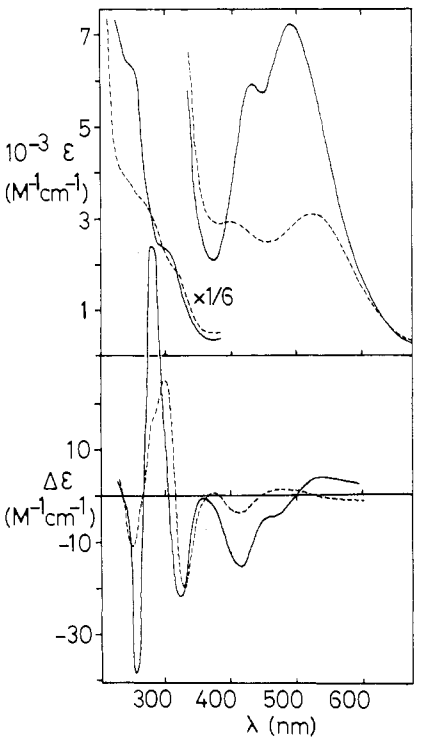

Figure 3. UV–visible absorption and circular dichroism spectra of $[\Lambda\text{-}Ni^{IV}((S)\text{-}Me_2L)]^{2+}$ (—), pH 2, and $[\Lambda\text{-}Ni^{III}((S)\text{-}Me_2L)]^{+}$ (- - -), pH 7, in aqueous perchlorate solution.

(26) IUPAC Rule 7.8: *Pure Appl. Chem.* **1971**, *28*, 75–80.

Table IV. $[Ni^{II}((S)\text{-}Me_2LH_2)](ClO_4)_2$: Positional and Thermal Parameters and Their Estimated Standard Deviations[a]

atom	x	y	z	B, Å²
Ni1	0.18388 (6)	0.77292 (5)	0.2866 (1)	2.68 (1)
O1	0.3917 (4)	0.7303 (3)	0.3117 (7)	4.6 (1)
O2	0.1891 (5)	0.7205 (3)	−0.0349 (6)	4.9 (1)
N1	0.3255 (4)	0.7799 (3)	0.2755 (7)	3.3 (1)
N2	0.2066 (4)	0.8679 (3)	0.1859 (7)	3.3 (1)
N3	0.0485 (4)	0.8124 (4)	0.2730 (8)	4.2 (2)
N4	0.1662 (5)	0.8062 (3)	0.5015 (7)	3.7 (2)
N5	0.1652 (4)	0.6773 (3)	0.3777 (7)	3.0 (1)
N6	0.1761 (5)	0.7049 (3)	0.1102 (7)	3.4 (1)
C1	0.3569 (5)	0.8391 (4)	0.2308 (9)	3.5 (2)
C2	0.4557 (5)	0.8552 (5)	0.219 (1)	7.3 (3)
C3	0.2876 (5)	0.8922 (4)	0.1934 (9)	3.3 (2)
C4	0.3156 (6)	0.9652 (4)	0.164 (1)	4.7 (2)
C5	0.1270 (6)	0.9085 (5)	0.140 (1)	4.5 (2)
C6	0.1378 (7)	0.9418 (6)	−0.007 (1)	6.7 (3)
C7	0.0484 (6)	0.8577 (5)	0.142 (1)	5.1 (2)
C8	0.0235 (6)	0.8506 (5)	0.404 (1)	4.8 (2)
C9	0.1044 (7)	0.8671 (5)	0.497 (1)	5.6 (2)
C10	0.1257 (7)	0.7474 (5)	0.584 (1)	4.8 (2)
C11	0.1648 (5)	0.6762 (4)	0.5366 (8)	3.5 (2)
C12	0.2590 (6)	0.6634 (5)	0.5916 (9)	5.0 (2)
C13	0.1479 (5)	0.6253 (4)	0.297 (1)	3.7 (2)
C14	0.1231 (7)	0.5507 (4)	0.346 (1)	5.5 (2)
C15	0.1576 (6)	0.6399 (4)	0.1375 (9)	3.1 (2)
C16	0.1470 (7)	0.5834 (5)	0.030 (1)	5.8 (3)
Cl1	0.6106 (2)	1.0474 (1)	0.2780 (3)	4.38 (4)
Cl2	0.1290 (2)	1.1430 (1)	0.2710 (3)	5.36 (6)
O3	0.6688 (6)	0.9876 (5)	0.292 (1)	9.1 (2)*
O4	0.6512 (5)	1.0915 (4)	0.175 (1)	8.0 (2)*
O5	0.584 (1)	1.0809 (9)	0.399 (2)	8.0 (4)*
O5′	0.623 (1)	1.0904 (7)	0.415 (2)	6.1 (3)*
O6	0.5263 (9)	1.0333 (7)	0.199 (2)	6.3 (3)*
O6′	0.535 (1)	1.013 (1)	0.282 (2)	9.9 (5)*
O7′	0.051 (1)	1.178 (1)	0.300 (2)	8.9 (5)*
O7	0.071 (1)	1.180 (1)	0.180 (2)	8.8 (5)*
O8	0.209 (2)	1.136 (1)	0.208 (3)	13.4 (7)*
O8′	0.155 (1)	1.128 (1)	0.125 (2)	10.4 (6)*
O9	0.1042 (6)	1.0762 (5)	0.323 (1)	9.8 (3)*
O10	0.152 (2)	1.188 (1)	0.388 (3)	12.9 (7)*
O10′	0.201 (1)	1.1685 (9)	0.331 (2)	8.1 (4)*

[a] Atoms marked with an asterisk were refined isotropically. Anisotropically refined atoms are given in the form of the isotropic equivalent thermal parameter defined as $^4/_3[a^2B_{11} + b^2B_{22} + c^2B_{33} + ab(\cos\gamma)B_{12} + ac(\cos\beta)B_{13} + bc(\cos\alpha)B_{23}]$.

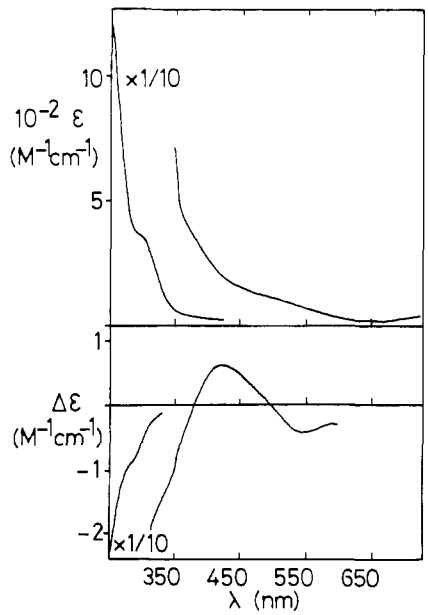

Figure 4. UV–visible absorption and circular dichroism spectra of $[\Lambda\text{-}Ni^{II}((S)\text{-}Me_2LH_2)]^{2+}$ at pH 3 in aqueous perchlorate solution.

(c) Kinetics and Mechanisms of Reduction of $[Ni^{IV}L]^{2+}$ by $[Co(pdta)]^{2-}$ and $[Co(cdta)]^{2-}$. The reductions of $[Ni^{IV}L]^{2+}$ by $[Co(pdta)]^{2-}$ and $[Co(cdta)]^{2-}$ parallel closely the corresponding reduction by $[Co(edta)]^{2-}$.[6] Thus, 2 equiv of the cobalt(II) complex are required in the reduction of nickel(IV) to nickel(II) and the reactions proceed in two readily distinguishable one-electron steps with formation of a nickel(III) intermediate. Details of the characterization of the intermediate may be found elsewhere.[16,27]

Table V. Pseudo-First-Order Rate Constants for the Reduction of $[Ni^{IV}L]^{2+}$ by $[Co(pdta)]^{2-}$ and $[Co(cdta)]^{2-}$ at 25.0 °C and 0.10 M Ionic Strength

pH 7.28[a]		
$10^4[[Co(pdta)]^{2-}]$,[b] M	$10^2(k_{obsd}(1))$, s^{-1}	$10^2(k_{calcd}(1))$,[d] s^{-1}
3.95	2.3 ± 0.2	1.9
15.8	6.5 ± 0.3	7.6
31.6	15.1 ± 1.0	15.2
55.3	25.7 ± 0.1	26.5
98.8	44.5 ± 1.4	47.4
pH 7.10[a]		
$10^4[[Co(cdta)]^{2-}]$,[c] M	$10^2(k_{obsd}(1))$, s^{-1}	$10^2(k_{calcd}(1))$,[d] s^{-1}
4.96	2.6 ± 0.6	2.2
9.9	4.7 ± 0.1	4.5
19.8	8.5 ± 0.2	8.9
29.8	12.4 ± 0.9	13.4
49.6	20.9 ± 0.4	22.3

[a] 1.5×10^{-2} M phosphate buffer. [b] $[[Ni^{IV}L]^{2+}] = 2.5 \times 10^{-5}$ M. [c] $[[Ni^{IV}L]^{2+}] = 1.8 \times 10^{-5}$ M. [d] Calculated by using data in the text.

Table VI. Pseudo-First-Order Rate Constants for the Reduction of $[Ni^{III}LH]^{2+}$ by $[Co(pdta)]^{2-}$ and $[Co(cdta)]^{2-}$ at 25.0 °C and 0.10 M Ionic Strength

pH[a]	$10^4[[Co(pdta)]^{2-}]$,[b] M	$10^3(k_{obsd}(2))$, s^{-1}	$10^3(k_{calcd}(2))$,[e] s^{-1}
4.20	5.1	4.55 ± 0.08	4.6
4.20	15.2	10.7 ± 0.1	10.9
4.20	30.5	15.1 ± 0.2	16.5
4.70	5.1	2.9 ± 0.1	2.2
4.70	20.2	7.8 ± 1.8	6.2
4.70	40.5	9.5 ± 0.1	9.0
4.70	70.8	12.8 ± 0.4	11.1
pH[a]	**$10^4[[Co(cdta)]^{2-}]$,[c] M**	**$10^3(k_{obsd}(2))$, s^{-1}**	**$10^3(k_{calcd}(2))$,[e] s^{-1}**
3.70[d]	14.2	13.9 ± 0.7	15.4
3.70[d]	24.8	21.6 ± 0.5	22.2
4.10	14.2	11.0 ± 0.6	11.6
4.10	24.8	17.5 ± 0.8	16.7
4.10	47.2	21.5 ± 0.1	23.1
4.60	4.7	2.9 ± 0.2	2.5
4.60	14.2	8.3 ± 0.3	6.1
4.60	24.8	11.5 ± 0.1	8.7
4.60	47.2	14.4 ± 0.7	12.1

[a] 3.0×10^{-3} M acetate buffer. [b] $[[Ni^{III}L]^+]_T = (2.6\text{–}3.4) \times 10^{-5}$ M. [c] $[[Ni^{III}L]^+]_T = (1.3\text{–}3.4) \times 10^{-5}$ M. [d] 1.5×10^{-2} M chloroacetate buffer. [e] Calculated by using data in the text.

The initial step in the reaction, reduction of $[Ni^{IV}L]^{2+}$, shows good first-order behavior (eq 1). The observed rate constants,

$$-d[[Ni^{IV}L]^{2+}]/dt = (k_{obsd}(1))[[Ni^{IV}L]^{2+}] \quad (1)$$

$k_{obsd}(1)$, show a first-order dependence on the concentration of $[CoY]^{2-}$ (where Y^{4-} is $pdta^{4-}$ or $cdta^{4-}$) (Table V), consistent with a simple bimolecular mechanism (eq 2). Second-order rate

$$[Ni^{IV}L]^{2+} + [CoY]^{2-} \rightarrow [Ni^{III}L]^+ + [CoY]^- \quad (2)$$

consants are 48 ± 3 M^{-1} s^{-1} for $[Co(pdta)]^{2-}$ and 45 ± 2 M^{-1} s^{-1} for $[Co(cdta)]^{2-}$, both at 25.0 °C and 0.10 M ionic strength.

The second step of the reaction, reduction of the nickel(III) intermediate, also follows pseudo-first-order kinetics (eq 3).

$$-d[Ni(III)]/dt = (k_{obsd}(2))[Ni(III)] \quad (3)$$

(27) Lappin, A. G.; Martone, D. P.; Osvath, P. *Inorg. Chem.*, in press.

Table VII. Kinetic Parameters for the Reductions of $[Ni^{IV}L]^{2+}$ and $[Ni^{III}LH]^{2+}$ by $[Co(edta)]^{2-}$, $[Co(pdta)]^{2-}$, and $[Co(cdta)]^{2-}$ at 25.0 °C and 0.10 M Ionic Strength

reductant	k_1,[a] M^{-1} s^{-1}	K,[b] M^{-1}	10^2k,[b] s^{-1}
$[Co(edta)]^{2-}$[c]	33	480	4
$[Co(pdta)]^{2-}$	48	310	7
$[Co(cdta)]^{2-}$	45	280	7

[a] Nickel(IV) reduction. [b] Nickel(III) reduction. [c] Reference 6.

However, the observed rate constants, $k_{obsd}(2)$, show a complex dependence on pH and $[[CoY]^{2-}]$ (Table VI). The data can be fit to the rate expression (eq 4) found in the corresponding reaction

$$k_{obsd}(2) = \frac{Kk[[CoY]^{2-}][H^+]}{(1 + K[[CoY]^{2-}])(K_H + [H^+])} \quad (4)$$

of $[Co(edta)]^{2-}$. The mechanism proposed, eq 5–7, involves the

$$[Ni^{III}LH]^{2+} \rightleftharpoons [Ni^{III}L]^+ + H^+ \quad K_H \quad (5)$$

$$[Ni^{III}LH]^{2+} + [CoY]^{2-} \rightleftharpoons [Ni^{III}LH^{2+},CoY^{2-}] \quad K \quad (6)$$

$$[Ni^{III}LH^{2+},CoY^{2-}] \rightarrow [Ni^{II}LH]^+ + [CoY]^- \quad k \quad (7)$$

more strongly oxidizing, protonated form of the nickel(III) as sole reactant. Electron transfer proceeds through a kinetically detectable precursor complex (eq 6). Some constraints can be put upon the acidity constant for nickel(III), K_H, which is known to be approximately 10^{-4} M.[6,16] Reasonable fits to eq 4 are obtained with $K_H = 7 \times 10^{-5}$ M, $K = 310 \pm 80$ M^{-1}, and $k = (7 \pm 1) \times 10^{-2}$ s^{-1} for $[Co(pdta)]^{2-}$ and $K_H = 6 \times 10^{-5}$ M, $K = 280 \pm 40$ M^{-1}, and $k = (7 \pm 1) \times 10^{-2}$ s^{-1} for $[Co(cdta)]^{2-}$. Rate constants calculated by using these parameters are presented in Table VI. The data are summarized together with the parameters for $[Co(edta)]^{2-}$ in Table VII.

Two comments on the data are relevant to this paper. First, there is a difference in the detailed mechanism between the reactions of the similarly charged $[Ni^{IV}L]^{2+}$ and $[Ni^{III}LH]^{2+}$, despite almost identical redox potentials and the likelihood that reactions of both species are outer-sphere in nature. This has been ascribed to the stabilization of the precursor complex in the case of nickel(III) by a strong hydrogen bond involving the protonated oxime group.[6] The nickel(IV) complex has no oxime protonation. That the kinetically detected precursor complex $[Ni^{III}LH^{2+},CoY^{2-}]$ is a true intermediate in the reaction and not a "dead-end" complex is supported by the magnitude of the second-order rates Kk for nickel(III) reduction, which should be a factor of 10 smaller than those for nickel(IV) reduction if the reactions obey Marcus theory.[27] They are, in fact, less than a factor of 2 different, indicating a significant kinetic advantage for the nickel(III) reaction resulting from the strong precursor complex.

Second, the rate parameters for reactions of $[Ni^{IV}L]^{2+}$ and $[Ni^{III}LH]^{2+}$ with $[Co(edta)]^{2-}$ and the two substituted derivatives are very similar despite the presence of substantial differences on the alkyl backbone of the reductants. This observation suggests that the $[CoY]^{2-}$ derivatives are oriented with the carboxylate face pointing toward the oxidant during the electron-transfer process.

(d) Stereoselectivity in the Reactions of $[\Lambda\text{-}Ni^{IV}((S)\text{-}Me_2L)]^{2+}$ and $[\Lambda\text{-}Ni^{III}((S)\text{-}Me_2LH)^{2+}$ with $[Co(pdta)]^{2-}$ and $[Co(cdta)]^{2-}$. The detection of stereoselectivity in the reaction of $[\Lambda\text{-}Ni^{IV}((S)\text{-}Me_2L)]^{2+}$ with $[Co(pdta)]^{2-}$ and $[Co(cdta)]^{2-}$ is a more complex process than with $[Co(edta)]^{2-}$. The experiments must be run with a significant excess of reductant since neither $[Co(pdta)]^{2-}$ nor $[Co(cdta)]^{2-}$ can racemize within the time frame of the electron-transfer process. Thus, addition of stoichiometric amounts of these reagents to solutions of $[\Lambda\text{-}Ni^{IV}((S)\text{-}Me_2L)]^{2+}$ leads to no stereochemical induction since both Δ and Λ isomers of the reductant are quantitatively oxidized. This problem does not arise with $[Co(edta)]^{2-}$, where the rate of racemization is ≥ 50 s^{-1} at 0 °C.[28]

Stereochemical induction in the overall reaction can be examined by reacting solutions of $[\Lambda\text{-}Ni^{IV}((S)\text{-}Me_2L)]^{2+}$ with excess $[Co(pdta)]^{2-}$ or $[Co(cdta)]^{2-}$. The nickel(III) step can be examined independently with use of $[\Lambda\text{-}Ni^{III}((S)\text{-}Me_2LH)]^{2+}$ as oxidant, and the results of both types of experiments are presented in Table VIII.

Table VIII. Results of Stereoselectivity Studies at 25.0 °C in Acetate Media and 0.10 M Ionic Strength

$[[Ni^{IV}((S)\text{-}Me_2L)]^{2+}]$, M	$[[CoY]^{2-}]$, M	pH	% stereoselectivity $[\Delta\text{-}CoY]^-$
	$[Co(edta)]^{2-}$		
6.8×10^{-4} [a,b]	6.8×10^{-4}	6.13	11.0 ± 0.5
6.8×10^{-4} [a]	1.36×10^{-3}	6.13	11.1 ± 0.5
6.8×10^{-4} [a]	1.36×10^{-3}	4.02	10.6 ± 0.5
9.4×10^{-5} [b]	9.4×10^{-5}	4.89	10.2 ± 1.0
9.3×10^{-5}	1.86×10^{-4}	4.89	11.0 ± 1.0
8.6×10^{-5}	9.1×10^{-4}	4.89	11.8 ± 1.0
	$[Co(pdta)]^{2-}$		
5.0×10^{-4} [c]	5.0×10^{-3}	4.00	11 ± 1
8.6×10^{-5}	9.1×10^{-4}	4.79	10.7 ± 1.0
1.7×10^{-4} [d]	1.7×10^{-3}	4.85	10.6 ± 1.0
	$[Co(cdta)]^{2-}$		
5.0×10^{-4} [c]	5.0×10^{-3}	4.00	12 ± 1
8.6×10^{-5}	9.1×10^{-4}	4.79	11.5 ± 1.0
1.7×10^{-4} [d]	1.7×10^{-3}	4.85	11.7 ± 1.0

[a] Reference 6. [b] Ni(IV) stereoselectivity only. [c] Using separation procedures in ref 6. [d] Ni(III) stereoselectivity only, using $[Ni^{III}((S)\text{-}Me_2LH)]^{2+}$.

Stereoselectivities in the nickel(IV) reduction step (eq 2) are 10.8%, 10.7%, and 11.4% for the reactions with $[Co(edta)]^{2-}$,[6] $[Co(pdta)]^{2-}$, and $[Co(cdta)]^{2-}$, respectively, while the corresponding values for the nickel(III) step (eq 6 and 7) are 11.6%, 10.6%, and 11.7%. In all cases the isomer induced in excess is the Δ form, and, despite differences in the mechanism of reduction of nickel(IV) and nickel(III), the extent of chiral induction is comparable. This does not contradict the proposed mechanisms, since stereoselectivity need not be related to the strength of precursor complex formation, but does suggest that the orientation of the complexes is similar in reactions of both nickel(IV) and nickel(III).

It is worthwhile considering the detailed mechanism of outer-sphere electron transfer in order to discuss possible origins of the stereoselectivity. Chiral induction requires some interaction between the reactants, and there are two ways in which this might be accomplished in the reaction of $[\Lambda\text{-}Ni^{IV}((S)\text{-}Me_2L)]^{2+}$ with a racemic mixture of enantiomers $[\Delta,\Lambda\text{-}CoY]^{2-}$.

1. There may be preferential precursor complex formation between $[\Lambda\text{-}Ni^{IV}((S)\text{-}Me_2L)]^{2+}$ and $[\Delta\text{-}CoY]^{2-}$ (any induced stereochemical preference or Pfeiffer effect may be ruled out in this case).

2. Electron transfer within the precursor $[\Lambda\text{-}Ni^{IV}((S)\text{-}Me_2L)^{2+},\Delta\text{-}CoY^{2-}]$ may be more rapid than within $[\Lambda\text{-}Ni^{IV}((S)\text{-}Me_2L)2^+,\Lambda\text{-}CoY^{2-}]$ due to preferential orbital overlap or to subtle differences in distances between the metal centers as a result of steric factors.

Differentiation of the effect between these two possibilities cannot be achieved by using the results of stereoselectivity studies of the electron transfer alone. However, some light may be cast on the precursor complex by examining stereoselectivity in the ion-pair interaction between the substitution-inert ions $[Ni^{IV}L]^{2+}$ and $[Co(edta)]^-$. This interaction differs from the precursor ion pair only with respect to the charge on the cobalt complex.

(e) Stereoselectivity in the Ion Pair between $[\Delta\text{-}Co(edta)]^-$ and $[Ni^{IV}L]^{2+}$. Circular dichroism spectra illustrating the partial resolution of $[Ni^{IV}L]^{2+}$ by cation-exchange chromatography using $[\Delta\text{-}Co(edta)]^-$ as eluent are shown in Figure 5. The mobility of the cation is determined in part by the strength of ion pairing within the mobile phase. Hence, the isomer that is eluted faster forms a stronger ion pair with $[\Delta\text{-}Co(edta)]^-$ than its enantiomer. The first eluted isomer has a circular dichroism spectrum very similar to that of $[\Lambda\text{-}Ni^{IV}((S)\text{-}Me_2L)]^{2+}$, indicating that the

(28) Blinn, E.; Pearce, C. F. V.; Wilkins, R. G. "Progress in Coordination Chemistry"; Cais, M., Ed.; Elsivier: Amsterdam, 1968; pp 135–137.

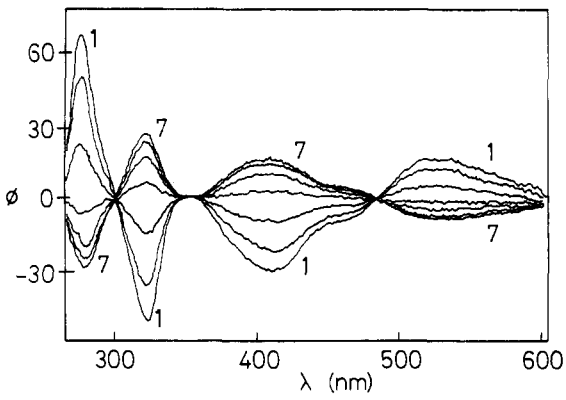

Figure 5. Circular dichroism spectra of solutions of $[Ni^{IV}L]^{2+}$ removed from a cation-exchange column after elution by $[\Delta(+)\text{-Co(edta)}]^-$. The ellipticity, ϕ, is in millidegrees, and the spectra have been normalized such that the absorbance of each solution at 500 nm is unity. The fastest eluted fraction is denoted 1 while the slowest fraction is denoted 7.

preferred ion pair is $[\Lambda\text{-}Ni^{IV}L^{2+},\Delta\text{-Co(edta)}^-]$.

(f) Interpretation of the Stereoselectivities. The stereochemical preference shown in the ion-pairing studies (Δ, Λ) is the same as the stereoselectivity in the electron-transfer reactions (Δ, Λ), suggesting that this electron-transfer stereoselectivity is attributable to preferential precursor complex formation between $[\Lambda\text{-}Ni^{IV}((S)\text{-}Me_2L)]^{2+}$ and $[\Delta\text{-CoY}]^{2-}$ and between $[\Lambda\text{-}Ni^{III}((S)\text{-}Me_2LH)]^{2+}$ and $[\Delta\text{-CoY}]^{2-}$. Hence, the preferred geometric arrangement serves as an intermediate in the electron-transfer process and not as a "dead-end" complex. Some comment on the similarity of the stereoselectivities of the nickel(IV) and nickel(III) reactions is required. It seems clear that the additional precursor complex stabilization in the latter reaction does not dramatically affect stereoselectivity. Presumably this is because the hydrogen-bonding interaction has little effect on the mutual orientation of the oxidant and reductant complexes or, stated more simply, because, in this case, hydrogen bonding does not affect the degree of chiral discrimination in the precursor complex.

By way of a contrast, Saito and co-workers note that stereoselectivity in the oxidation of $[Mo^{V}_2O_4((R,S)\text{-pdta})]^-$ by $[\Delta\Delta\text{-}(en)_2Co(\mu\text{-}O_2^-,NH_2)Co(en)_2]^{4+}$ is dependent on the magnitude of the kinetically detected ion-pairing consants. A stereoselectivity of around 9% favoring interaction with the (*R*)-pdta isomer is found for ion pairing whereas the electron-transfer component shows smaller selectivity favoring the (*S*)-pdta isomer. Such results may indicate that the kinetically detected ion pair is a "dead-end" complex.

There is limited information available on stereoselectivity in associations between complex ions in solution.[29-31] The basis of chiral discrimination rests with differences in chirality of the C_3 (or pseudo-C_3) and C_2 (or pseudo-C_2) axes of an octahedral complex. For a Δ isomer, this is designated $P(C_3),M(C_2)$ while a Λ isomer has the opposite designation $M(C_3),P(C_2)$.[32] In interactions between complex ions, *PP* or *MM* orientations are apparently preferred.[29]

This approach may be applied to the association of $[\Lambda\text{-}Ni^{IV}L]^{2+}$ with $[\Delta\text{-Co(edta)}]^{2-}$. The $[Co(edta)]^{2-}$ ion generally prefers to use a pseudo-C_3 axis in chiral discrimination, presenting a face with three carboxylate oxygens.[29] The present results support this proposal in that there is little effect on rate and stereoselectivity parameters with changing substituents on the alkyl backbone of the ligand in $[Co(edta)]^{2-}$. It follows that an interaction with the C_2 axis of the nickel(IV) complex is preferred and an orientation with both oxime groups directed toward $[Co(edta)]^{2-}$ seems a reasonable representation of the electron-transfer precursor complex. In the reaction of $[Ni^{III}((S)\text{-}Me_2LH)]^{2+}$, this would allow stabilization by hydrogen bonding between the oxime of the nickel complex and carboxylate groups of the cobalt complex.

Table IX. Stereochemical Preferences in Electron-Transfer and Ion-Pairing Studies

reagents	ET[a]	IP[b]	ref
$[Os(bpy)_3]^{3+}$ + $[Co(edta)]^{2-}$	$\Delta\Delta$		2
$[Ru(bpy)_3]^{3+}$ + $[Co(edta)]^{2-}$	$\Lambda\Delta$		2
$[Co(bpy)_3]^{3+}$ + $[Co(edta)]^{2-}$	$\Delta\Delta$		2
$[Fe(bpy)_3]^{3+}$ + $[Co(edta)]^{2-}$	$\Lambda\Delta$		2
$[Fe(phen)_3]^{3+}$ + $[Co(edta)]^{2-}$	$\Lambda\Delta$		2
$[Co(edta)]^-$ + $[*Ru(bpy)_3]^{2+}$	$\Lambda\Delta$		5
$[Co(acac)_3]$ + $[*Ru(bpy)_3]^{2+}$	$\Lambda\Delta$[c]		4
$[Co(phen)_3]^{3+}$ + $[Co(acac)_3]^-$	$\Lambda\Delta$[d]		33
$[Co(acac)_3]$ + $[Ni(phen)_3]^{2+}$		$\Delta\Delta$	34
$[Co(edta)]^-$ + $[Co(en)_3]^{2+}$	$\Delta\Delta$		2
$[Co(edta)]^-$ + $[Co(en)_3]^{3+}$		$\Lambda\Delta$	29
$[Ni^{IV}L]^{2+}$ + $[Co(edta)]^{2-}$	$\Lambda\Delta$		6
$[Ni^{III}LH]^{2+}$ + $[Co(edta)]^{2-}$	$\Lambda\Delta$		6
$[Ni^{IV}L]^{2+}$ + $[Co(edta)]^-$		$\Lambda\Delta$	this work
$[Ni^{IV}L]^{2+}$ + $[Co(pdta)]^{2-}$	$\Lambda\Delta$		this work
$[Ni^{III}LH]^{2+}$ + $[Co(pdta)]^{2-}$	$\Lambda\Delta$		this work
$[Ni^{IV}L]^{2+}$ + $[Co(cdta)]^{2-}$	$\Lambda\Delta$		this work
$[Ni^{III}LH]^{2+}$ + $[Co(cdta)]^{2-}$	$\Lambda\Delta$		this work

[a] Electron transfer. [b] Ion pairing. [c] It is possible that these results may be explained by a $\Delta\Delta$ preference in the back-reaction $[Ru(bpy)_3]^{3+}$ + $[Co(acac)_3]^-$. [d] It is unclear whether these results are best described as a Pfeiffer effect or a stereoselective electron transfer.

(g) Implications for Other Studies. A summary of the published data on stereoselectivity in electron transfer together with selected ion-pairing data is presented in Table IX. It can be seen that, apart from the present work, the correlation of electron-transfer and ion-pair stereoselectivities is possible in only two cases. In both these cases, stereoselectivity in the ion pair is the opposite of that found in the electron-transfer reaction, suggesting that the dominant ion pair is a "dead-end" interaction.

The majority of stereoselectivity studies have been carried out between complexes of the type $[M(bpy)_3]^{3+}$ or $[M(phen)_3]^{3+}$ and $[Co(edta)]^{2-}$, with no well-defined trends. Clearly ion-pairing information in these systems is required before any rationalization can be attempted. Experiments in which $[\Delta\text{-Co(edta)}]^-$ was used as an eluent for cation-exchange studies involving racemic $[Co(phen)_3]^{3+}$ resulted in minimal resolution, not surprising since the mode of association between $[Co(edta)]^-$ and $[Co(phen)_3]^{3+}$ is much more poorly defined than with $[Co(en)_3]^{3+}$ or $[Ni^{IV}L]^{2+}$, where possibilities for hydrogen bonding exist.

These studies serve to show that orientation restrictions in outer-sphere electron-transfer reactions can be significant. Though information of this sort can be implied[35] from work term calculations in the Marcus analysis of electron-transfer rates, stereoselectivity studies, where applicable, have much greater sensitivity and have the potential for more detailed interpretation.

Acknowledgment. This work was supported by the National Science Foundation (Grant No. CHE84-06113) and the Jesse H. Jones Faculty Research Fund of the University of Notre Dame. Thanks are also due to CAPES, Brasilia, Brazil, for a Maintenance grant to M.C.M.L.

Registry No. $[Ni^{II}((S)\text{-}Me_2LH_2)](ClO_4)_2$, 99395-48-9; $[Ni^{IV}((S)\text{-}Me_2L)]^{2+}$, 99342-18-4; $[Ni^{III}((S)\text{-}Me_2L)]^{+}$, 99342-21-9; $[Ni^{IV}L](ClO_4)_2$, 99342-20-8; $[Ni^{III}LH]^{2+}$, 99327-70-5; $[Co(pdta)]^{2-}$, 52582-07-7; $[Co(cdta)]^{2-}$, 28161-91-3; $[\Delta(+)_{546}\text{-Co(edta)}]^-$, 27829-16-9; $[IrCl_6]^{2-}$, 16918-91-5; $[Co(edta)]^{2-}$, 14931-83-0.

Supplementary Material Available: Listings of calculated hydrogen atom positions (Table X), general temperature factor expressions (B_{ij}'s) (Table XI), and observed and calculated structure factors (Table XII) (25 pages). Ordering information is given on any current masthead page.

(29) Sakaguchi, U.; Yamamato, I.; Izumoto, S.; Yoneda, H. *Bull. Chem. Soc. Jpn.* **1983**, *56*, 153-156.
(30) Sakaguchi, Y.; Yamamoto, I.; Izumoto, S.; Yoneda, H. *Bull. Chem. Soc. Jpn.* **1983**, *56*, 1407-1409.
(31) Tatehata, A.; Liyoshi, M.; Kotsuji, K. *J. Am. Chem. Soc.* **1981**, *103*, 7391-7392.
(32) Mason, S. F. "Molecular Optical Activity and the Chiral Discriminations"; Cambridge University Press: Cambridge, England, 1982; p 15.
(33) Miyoshi, K.; Wada, Y.; Yoneda, H. *Chem. Lett.* **1977**, 319-320.
(34) Yamamoto, M.; Iwamoto, E.; Kozasa, A.; Tatemata, K. *Inorg. Nucl. Chem. Lett.* **1980**, *16*, 71-74.
(35) See for example: Phillips, J.; Haim, A. *Inorg. Chem.* **1980**, *19*, 76-79.